Signature: © Pol J Radiol, 2009; 74(2): 28-34

Polish Journal of Radiology
www.PolRadiol.com
ORIGINAL ARTICLE

Received: 2009.03.12
Accepted: 2009.03.24

Quantitative analysis of 3D US images in the relationship with liver lesion diagnosis

Eugeniusz Rokita[1,2], Grzegorz Tatoń[1], Marek Sierżęga[3], Jan Kulig[3], Andrzej Urbanik[4]

[1] Department of Biophysics, Jagiellonian University Medical College, Cracow, Poland
[2] Institute of Physics, Jagiellonian University, Cracow, Poland
[3] 1st Department of General and GI Surgery, Jagiellonian University Medical College, Cracow, Poland
[4] Chair and Department of Radiology, Jagiellonian University Medical College, Cracow, Poland

Author's address: Grzegorz Tatoń, Department of Biophysics, Jagiellonian University Medical College, Cracow, e-mail: mmtaton@cyf-kr.edu.pl

Source of support: Work supported by the Polish State Committee for Scientific Research with grant no 6 P05C 015 21

Summary

Background: The aim of the study was to apply a computer aided analysis of the three-dimensional (3D) ultrasound images for the diagnosis of focal liver lesions.

Material/Method: Patients with various hepatic changes were examined using standard US unit equipped with a transducer positioning system based on the magnetic field sensor. The data were imported by the graphical workstation and processed. The computer analysis comprised 3D image segmentation as well as the lesion volume and echogeneity determination. Moreover, a set of parameters was calculated to quantify morphology and texture of the lesions.

Results: The collected results confirmed that calculations of lesion volume and echogeneity as well as quantification of the morphological features have a limited value in the diagnosis of liver tumors. In contrast, the quantification of selected texture features of the 3D liver images enables differentiation between malignant and benign tumors. The best parameters to distinguish between different types of the liver lesions are angular second moment and entropy.

Conclusions: The results suggest that quantification of the texture features offers the supplementation of the routine US approach to the liver lesion diagnosis by a new quantitative tool.

Key words: **ultrasonic imaging • three-dimensional imaging • image analysis • liver lesions**

PDF file: http://www.polradiol.com/fulltxt.php?ICID=887301

Background

In the last two decades two-dimensional (2D) ultrasound (US) imaging has made tremendous progress in obtaining important diagnostic information [1]. Despite all the advances in US imaging techniques [2–4] detection and characterization of liver tumors still represent the challenge to 2D imaging methods. For example, the reported sensitivity of 2D US for the detection of liver metastases varies from 40% to 70% [5]. The main limitations are high operator dependency and low specificity.

Over the past few years, research investigators and commercial companies have further advanced ultrasound techniques with the development of three-dimensional (3D) US equipment [6–8]. In a 3D US examination, the 2D images are combined to form a 3D image of the anatomy and pathology. Theoretically, this image can then be viewed, manipulated and quantitatively measured as well as 2D cross-sectional image can be generated in any orientation. Therefore, 3D US seems to overcome the limitations of 2D US imaging.

State-of-the-art 3D US imaging is limited to the acquirement of a "pretty picture" and to the determination of the organ volumes. The techniques does not provide, at present, additional diagnostic information. Since the reconstruction of 3D images is the computer aided technique, the raw data are stored in the digital form. Therefore, the

advanced computer processing of the 3D US images seems to be natural extension of the routine approach. The aim of this paper is to highlight the various issues related to computer aided analysis of the 3D US images of focal liver lesions.

Material and Methods

The present study included 25 subjects (17 males and 8 females). Informed consent was obtained from all subjects prior to US and computed tomography (CT) examinations. Mean age was 60.1 y (range 41–83 y). Because of the methodical character of the project patients with different alternations were chosen in order to check the abilities of tested methods in different conditions. Malignant as well as benign lesions were observed within the investigated group: malignant liver changes – 15 cases (colorectal cancer metastasis – 9, gastric cancer metastasis – 3, hepatocellular carcinoma – 3), benign liver changes – 10 cases (cyst – 6, focal steatosis – 4). The diagnosis was confirmed with the fine needle aspiration biopsy and/or the CT examinations.

The 2D US examinations were performed with the use of Hitachi EUB-525 US unit. All images were obtained by using 3.5 MHz transducer. The same US unit was used in the 3D investigations. In this part of the study the device was equipped with the 3D imaging system delivered by Echotech 3D Imaging Systems (Hallbergmoos, Germany). The 3D US images were collected using a free-hand scanning approach. A magnetic field sensor with six degree of freedom was applied to mark the transducer position. Data processed preliminary by the 3D imaging system software were exported as the series of TIFF files, subsequently imported by the graphical workstation and processed.

The routine CT examinations were done with the use of Siemens Somatom Sensation 10 multi-slice system. Data saved as DICOM files were also imported into the graphical workstation in order to reconstruct the 3D images and to perform volume measurements.

DELL Precision Workstation 530MT equipped with two Intel Xeon 2.8 GHz processors and 2 GB f RAM was used for data processing. Specially developed dedicated software created in our laboratories was used for data import, reconstruction and analysis.

Computer aided analysis of the 3D US data begins with the image segmentation. On the basis of performed tests the modified version of the split-and-merge algorithm [9] was used for isolating the lesion in a digital image. It should be clearly pointed out that we did not use any image enhancement methods before segmentation. Such approach was selected to avoid any changes in the internal structure of the lesion. The split-and-merge method is a top-down technique which begins with the entire field of view (FOV). The well defined image property is selected as criteria to decide, whether to FOV is uniform or not. If the criterion is not met the FOV is divided into eight cuboids. Then each of cuboids is examined in the same way and subdivided, if necessary up to the level of one voxel. Each dividing step is followed by a merge step. In the merge step adjacent cuboids are connected if they are similar according to the pre-selected criterion.

In our implementation of the split-and-merge algorithm we choose the standard deviation of the brightness histogram and the size of the cuboid as the criteria to subdivide cuboids. The threshold values of both quantities are two adjustable parameters. It should be noted that the size of the cuboid below which the division step is not performed determines the roughness of the region border. The lowest possible value (1 voxel) was fixed in the calculations. In the merge step the classification of the cuboids was based on their mean brightness.

Next, the determination of the lesion echogeneity was performed. The degree of internal echogeneity was accessed by comparing the lesion with the surrounding liver tissue. The simplest technique of echogeneity calculation was applied. The method relies on the calculation of the average grey level within the lesion and within the surrounding liver tissue. The parameter, equals to the ratio of both average values was applied to quantify the echogeneity of the lesion. Additionally, the volume of the lesion was calculated by simple summation of all voxels within the segmented region. The volume determination was performed for US and CT images. Since the real dimensions of investigated structures were not known the CT results were treated as the most reliable data ("gold standard") and the outcomes of the 3D US method were compared to the CT results.

The final step of the computer aided analysis was the quantitative description of features to characterize the hepatic lesions. The first group of quantities described the morphology of the lesion. As the preliminary step of the morphological feature extraction the lesion was approximated by a convex solid body and by an ellipsoid centered at the center of the lesion. It should be noted that fitting of the ellipsoid, results in the description of the lesion by three parameters, equal to the three main axes of the ellipsoid. In the present studies the following quantitative measures of the morphological features were calculated for 3D US images: (1) compactness (COM) defined as S_C/S_L where S_C and S_L are the surface of the convex solid body and the lesion respectively, (2) filling ratio (FR) equals to V_L/V_C, where V_L and V_C are the volumes of the lesion and the convex solid body respectively, (3) eccentricity (EC) given as (maximal axis of the ellipsoid)/(minimal axis of the ellipsoid). It should be noted that COM and FR give values between and 1 while EC is, by definition, bigger or equal to 1.

To extract texture characteristics spatial grey level dependency (SGLD) matrices were calculated. The (j,h)th element of the SGLD matrix for an object is the number of times, divided by the number of voxel pairs contributing to SGLD, that gray levels i and j occur in two voxels separated by the distance d in the image. The size of the SGLD matrix equals the number of grey levels ($N \times N$). To avoid a large SGLD matrix, the number of grey levels was reduced to 128 after histogram equalization. A number of SGLD matrix-based parameters have been defined and tested [10]. In the present studies three measures are extracted from SGLD matrices: entropy (EN), angular second moment (ASM) and contrast (CON). Assuming that grey scale has N shades of grey and p_{ij} marks (i,j)th element of the SGLD matrix:

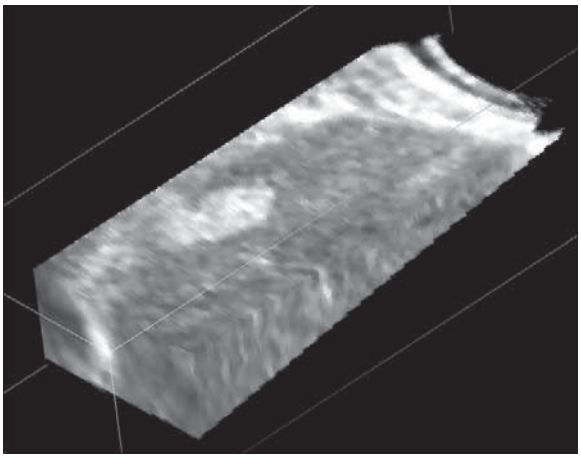

Figure 1. 3D US imaging study of a 62-year-old male with a liver metastases.

Figure 2. Conventional 2D US showing the lesion presented in Figure 1. Scan from a 62-year-old male with a liver metastases shown.

$$EN = -\sum_{i=0}^{N-1}\sum_{j=0}^{N-1} p_{ij} \ln(p_{ij}) \quad (1)$$

$$ASM = -\sum_{i=0}^{N-1}\sum_{j=0}^{N-1} p_{ij}^{2}) \quad (2)$$

$$CON = -\sum_{i=0}^{N-1}\sum_{j=0}^{N-1} (i-j)^{2} p_{ij} \quad (3)$$

It should be pointed out that the SGLD matrix is a probability of grey level i and j for two voxels with defined separation in the image. The separation is described in terms of distance d and angle Θ. For each (d,Θ) pair one SGLD matrix was calculated. In the present studies the SGLD matrices are constructed for the distances d=(1÷15) voxels and for three perpendicular directions.

Results

An example of 3D US image is presented in Figure 1. The software provides three perpendicular planes which are displayed simultaneously. The results of routine 2D US and CT examinations are shown in Figures 2 and 3 for comparative purposes. In Figure 4 the results of partitioning of a 3D US digital image is given. The surface rendering technique was used to visualize the focal liver lesion.

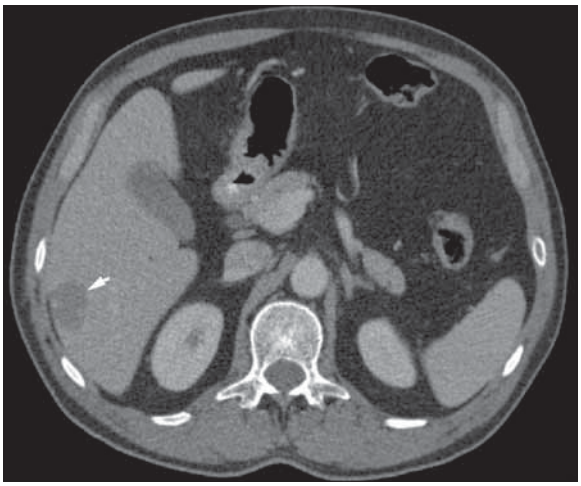

Figure 3. 2DCT imaging study of a 62-year-old male with a liver metastases. Arrow marks the focal liver lesion shown in Figure 1.

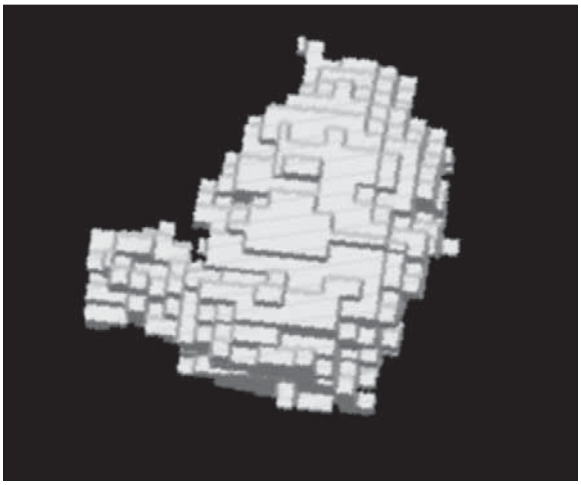

Figure 4. Automated segmentation of the digital image presented in Figure 1. The surface rendering technique was used to visualize the lesion.

After the lesion is segmented, the voxels were summed and the matrix voxel scaling factor was applied to determine the volume. In the examined subjects the volumes determined on the basis of 3DUS images ranged from 6.8 cm^3 to 156 cm^3, i.e. were typical for the liver lesions (Table 1). The US volumes correlate well with the values extracted from CT images (correlation coefficient =0.87). The observed differences do not surpass 10%. For example, for the lesion presented in Figure 1 the US and CT volumes equal to 18.7 cm^3 and 18.2 cm^3, respectively.

The results of the echogeneity quantification are given in Table 1. Since the malignant lesions (metastasis – MET, hepatocellular carcinoma – HCC) may be hypo- or hyperechoic the observed values of the echogeneity (Table 1) are smaller or bigger than 1. In the case of the cyst (CYS) and the focal liver steatosis (FLS) the echogeneity is always

Table 1. Quantitative description of the focal liver lesions. Values of parameters (Mean ±SD) and ranges for 4 groups of subjects (MET – metastases, HCC – hepatocellular carcinoma, CYS – cyst, FLS – focal liver steatosis) are given.

Parameter	Volume (cm^3)		Echogeneity	
Group	Mean ±SD	Range	Mean ±SD	Range
MET	51.5±43.9	6.8÷156	0.94±0.21	0.67÷1.40
HCC	55.0±26.9	28.5÷91.8	0.91±0.11	0.81÷1.05
CYS	45.8±19.6	8.5÷70.1	0.67±0.15	0.53÷0.75
FLS	44.7±25.4	14.6÷80.9	0.75±0.09	0.69÷0.84

Table 2. Morphological measures applied for the quantitative description of the focal liver lesions. Values of parameters (Mean ±SD) for 4 groups of subjects (MET – metastases, HCC – hepatocellular carcinoma, CYS – cyst, FLS – focal liver steatosis) are given.

Parameter	Compactness		Filling ratio		Eccentricity	
Group	Mean ±SD	Range	Mean ±SD	Range	Mean ±SD	Range
MET	0.79±0.08	0.66÷0.91	0.55±0.12	0.37÷0.72	5.0±1.5	2.8÷7.9
HCC	0.80±0.07	0.71÷0.88	0.57±0.11	0.42÷0.69	6.5±1.8	4.7÷9.0
CYS	0.90±0.04	0.89÷0.94	0.62±0.10	0.49÷0.75	7.2±1.3	5.3÷9.8
FLS	0.90±0.03	0.85÷0.93	0.66±0.10	0.53÷0.78	5.9±1.6	4.1÷8.5

smaller than 1 what confirms the anechoic or hypo-echoic US appearance of the benign liver lesions.

The quantitative description of the morphology of the liver lesions is summarized in Table 2. The presented measures characterize quantitatively different features of the lesions. It should be emphasized that the ranges of parameters in Table 2 overlap. For the statistical inference the malignant (MET and HCC) and benign (CYS and FLS) tumors were pooled together. The mean values of the parameters equal to: COM = 0.79±0.08 and 0.90±0.03, FR=0.55±0.12 and 0.63±0.10, EC=5.3±1.7 and 6.7±1.6, for malignant and benign groups respectively. Although trends may be recognized, the observed differences are not statistically significant (ANOVA, p=0.05). It should be pointed out that the parameters presented in Table 2 are extracted from 3D images.

Examples of the texture quantification are given in Figures 5 and 6. The calculations were performed with different distances d and for three perpendicular directions. To represent each texture feature of the 3D image by one parameter the average values were calculated for the voxel separation d in the range of (6÷15) voxels. The limits of the ranges was selected assuming that the parameters values are independent of d. The final results of the quantitative texture analysis are given in Table 3. It should be pointed out that the average values were obtained on the basis of 30 SGLD matrices (three directions times 10 d values). The data in Table 3 revealed that ASM values enable distinguishing of all groups under considerations because the ranges of the values do not overlap. The EN values offer the possibility to separate malignant (MET and HCC) and benign (CYS and FLS) lesions while in case of the CON the overlap of the ranges were observed.

Discussion

Although clinical application of 3D US imaging is growing, currently the technique is mostly applied to quantify the volumes and to provide "pretty pictures" of organs and lesions [11–13]. It pertains also to the use of the contrast enhanced agents. We have presented an attempt to assess automated quantification of the 3D US images of the focal liver lesions. The first step of the proposed evaluation method relies on the 3D image reconstruction and lesion visualization, i.e. overlaps with the widespread clinical use of the 3D US technique. Many reconstruction algorithms and display methods (surface rendering, multi-planar reformatting, volume rendering) are currently used [6,7]. The optimal approach to examine and interpret patient data has yet to be established. The best visualization method is operator-dependent. Therefore, variety of visualization tools should be available, to assist the physician to optimize examination.

After the reconstruction is completed the 3D US images have to be segmented. Methods for performing segmentation vary widely depending on the specific application and imaging modality. There is currently no single segmentation method that yields acceptable results for every medical image. In case of 3D US, high levels of speckling make accurate segmentation difficult. Automated, semi-automated and manual segmentation techniques are used to isolate focal lesions from noisy backgrounds [14–16]. On the basis of performed tests we applied the split-and-merge algorithm for segmentation of 3D US liver images. After adjustment of three parameters the fully automated segmentation was performed. The correctness of the algorithm was confirmed by the presence of the liver lesions both in 3D US and CT images of all subjects under considerations.

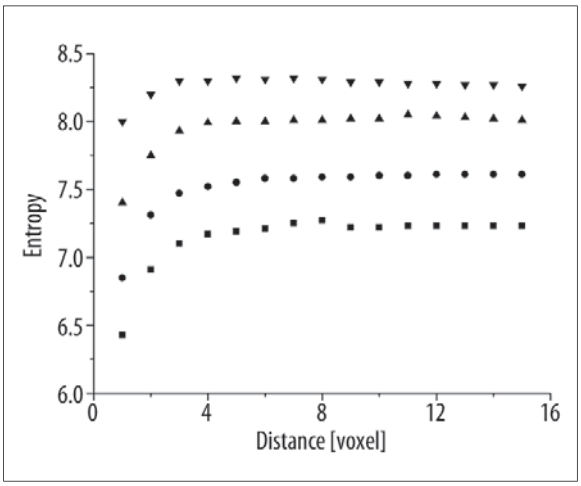

Figure 5. The texture quantification for the focal liver lesions. The entropy vs distance between voxels is presented. The average values in three perpendicular directions for 4 groups of subjects (metastases – ▼, hepatocellular carcinoma – ▲, cyst – ●, focal liver steatosis – ■) are given.

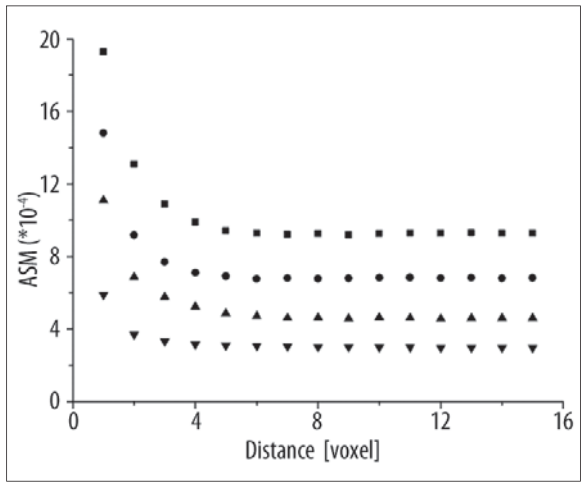

Figure 6. The texture quantification for the focal liver lesions. The angular second moment (ASM) vs distance between voxels is presented. The average values in three perpendicular directions for 4 groups of subjects (metastases – ▼, hepatocellular carcinoma – ▲, cyst – ●, focal liver steatosis – ■) are given.

Table 3. Texture measures applied for the quantitative description of the focal liver lesions. Values of parameters (Mean±SD) and ranges for 4 groups of subjects (MET – metastases, HCC – hepatocellular carcinoma, CYS – cyst, FLS – focal liver steatosis) are given.

Parameter	Entropy		Angular second moment (10-4)		Contrast	
Group	Mean ±SD	Range	Mean ±SD	Range	Mean ±SD	Range
MET	8.3±0.2	7.9÷8.5	3.0±0.4	2.4÷3.7	541 ± 19	396÷717
HCC	8.0±0.1	7.9÷8.1	4.6±0.3	4.2÷4.9	288±24	252÷324
CYS	7.6±0.1	7.5÷7.7	6.8±0.3	6.3÷7.3	238±18	226÷316
FLS	7.2±0.1	7.1÷7.3	9.3±0.3	9.1÷9.5	195 ± 8	192÷199

Moreover, the volumes determined on the basis of 3D US and CT images correlate well.

Although the segmentation facilities the visual assessment of the lesion, the goal of the computer aided processing relies on the labeling of the region. For focal liver lesions, labeling is the process of assigning a meaningful designation to each region as being malignant or benign. As may be expected the volume of the lesion as well as the average echogeneity (Table 1) are useless for this purpose. The volume of the lesion is important in the planning of the treatment and for the assessing treatment while the average echogeneity has only a supplementary diagnostic value. In routine clinical practice the liver lesions are described qualitatively. For example, liver cyst is characterized as the round, anechoic lesion possessing the smooth well-defined borders which differs in echogeneity in comparison with the surrounding liver tissue [1]. More variable and non-specific description is correlated with US appearance of the malignant tumors [17]. In the present studies a trial was undertaken to assess quantitatively the morphology and texture of the focal liver lesions.

The morphological features have come into common use because they are important in a variety of pattern recognition problem. For example, morphological features have been used in a range of mammographic studies [18,19] to select micro-calcifications. Many quantities are used to quantify morphology of the lesions [14,15]. We limited ourselves to three parameters that may be considered as the representative examples. The compactness and the filling ratio are measures of the surface complexity. A lesion possessing the complicated border could be expected to have smaller COM and FR values than a tumor characterized by the smooth surface. The eccentricity is a compact representation of a lesion shape. Round lesions are characterized by the EC value close to 1 while for elongated regions EC should be much bigger than 1. The collected results (Table 2) do not confirm the usefulness of the morphological feature quantification in the diagnosis of focal liver lesions. Probably, it results from the fact that malignant and benign liver tumors have non-specific shape and border characteristics. Moreover, the border structure may be influenced by the segmentation procedure.

Contrary to morphological features, the quantitative description of the lesion texture has an important diagnostic value. The texture analysis method was applied previously in clinical research to detect pathology [20–23]. The most important problem in the image texture quantification

is the selection of the optimal d value [24,25]. In our studies the problem was solved by calculations of the mean values over the carefully selected range of the distance d. The selection of the range was based on the assumption that for the optimal distance the parameter is independent of d. It should be emphasized that the image texture is quantified by one parameter which may be easy calculated in the routine clinical practice.

A great number of parameters can be calculated on the basis of the SGLD matrix [10,26,27]. We limited ourselves to two parameters (AFM, EN) which offer the best differentiation of the focal liver lesions. Moreover, one quantity (CON) which is useless for this purpose was considered for comparative purposes. The parameters included into considerations may be correlated with the internal structure of the lesion.

The entropy is a measure of the disorder of gray voxel values. Low values of EN are obtained when SGLD matrix elements are very different from each other. It corresponds to the image which contains small number of gray levels. Higher values of EN indicate the SGLD matrix is equal what means that the lesion is composed of voxels characterized by many different shades of gray. In agreement with commonly accepted opinion [5,17], for malignant liver tumors (MET, HCC) the EN values should be bigger than for the benign lesions (CYS,FLS). The results of our studies (Fig. 5) showed that, when the EN values are calculated for focal liver lesions, malignant and benign nature of the tumor may be easy recognized since the ranges of EN values do not overlap (Table 3).

The angular second moment is used to characterize the homogeneity of the lesion. In a homogeneous image there are few (at the limit one) dominant gray levels and the SGLD matrix contains only few elements of a large magnitude. In contrast, in a less homogeneous image there are many entries in the SGLD matrix of smaller magnitude and the ASM is smaller in magnitude. Hence, homogenous lesions (CYS, FFL) are characterized by bigger ASM values than malignant ones (MET, HCC). It may be concluded that ASM values enable separation of all groups distinguished in our studies since the ranges of parameters do not overlap (Table 3). Although, the small number of subjects in each group limits the diagnostic value of the latter conclusion, the significant difference between malignant and benign groups is worthy of remembrance.

The contrast is a measure of the amount of local variation in the image. A low values of contrast results from uniform images without pronounced variation of the gray levels whereas images with large local variation produce a high value. In our studies the ranges of the CONT values for CYS and HCC groups overlap. Probably, it results from the fact that cysts complicated by infection or hemorrhage may have septations and/or internal debris. Therefore, the US image of the cyst may be characterized by bigger local variation than that of the focal fatty lesion. What is more, the local variations in the images of the cyst and the HCC tumor may be very similar in some cases.

In summary, it may be stated that the applied parameters enable quantitative characterization of the liver lesions. Since the parameters ASM and EN are highly correlated [25] only one of this pair would be necessary in a classification task. Since the ranges of the parameter values do not overlap, the calculation of the ASM and/or EN values can assist the physician in finding the correct diagnosis. A special remark is necessary to depict the importance of the 3D imaging since, 2D US remains the first imaging method. The differences between 3D and 2D analyses rely mostly on the number of the SGLD matrices used in the calculations. In the other words, 3D US imaging offers much higher precision of the estimation of the parameters than the 2D US method does. Moreover, in the case of the 2D image the texture in one direction is not included in the considerations. Therefore, a pronounced error may be accounted. A possible error may be compared to the estimation of the solid body volume on the basis of a cross-section area.

It should be also emphasized that our studies are limited by two problems. First, the internal structure of the lesions is likely to be machine specific. The adjustment of the US unit may influence the image appearance and the absolute values of the parameters. The relationships between values of the texture parameters observed for different groups should, however, remain unchanged. Second, the number of patients involved in the studies was limited. Therefore, a trial encompassing bigger groups of different malignant tumors is necessary.

Conclusions

US liver imaging is usually undertaken to search for primary or metastatic liver disease. The 3D technology is a certainty and will continue to have a major impact on US application for the foreseeable future. The success of 3D US methods will depend on providing performance that exceeds that of 2D US. We introduced a new quantitative approach to 3D US liver imaging. The proposed method is based on the digital image analysis. It was confirmed that the quantification of the selected texture features (angular second moment and entropy) of the 3D US images may be useful in the liver lesion characterization. Since the ranges of texture parameters do not overlap, the separation of different pathologies may be based on the parameter values. The statistical methods were not applied to support the conclusions. With the use of the proposed method, the visual human experience is supplemented by the quantitative tool. It is also worthy to note that the reconstruction and data processing can be conducted with the use of a standard PC, so low-costs investment results in the introduction of advanced and useful diagnostic possibilities.

References:

1. Sahani D, Kalva S: Imaging the liver. Onkologist, 2004; 9: 385–97
2. Lewin P: Quo Vadis medical ultrasound? Ultrasonics, 2004; 42: 1–7
3. Hoeffel C, Mulé S, Romaniuk B et al: Advances in radiological imaging of gastrointestinal tumors. Crit Rev Oncol Hematol, 2009; 69: 153–67
4. Maruyama H, Yoshikawa M, Yokosuka O: Current role of ultrasound for the management of hepatocellular carcinoma. World J Gastroenterol, 2008; 14: 1710–19
5. Paulson E: Evaluation of the liver for metastatic disease. Semin Liver Dis, 2001; 21: 225–36

6. Fenster A, Downey D, Cardinal H: Three-dimensional ultrasound imaging. Phys Med Biol, 2001; 46: R67–99
7. Mor-Avi V, Sugeng L, Lang RM: Real-time 3-dimensional echocardiography: an integral component of the routine echocardiographic examination in adult patients? Circulation, 2009; 119: 314–29
8. Polaków J, Janica J, Serwatka W et al: Value of three-dimensional sonography in biopsy of focal liver lesions. Hepatobiliary Pancreat Surg, 2003; 10: 87–89
9. Russ J: The image processing handbook. CRC Press, Boca Raton, 1995
10. Haralik R: Statistical image texture analysis. In: Fu K (ed.): Handbook of pattern recognition and image processing. Academic, Orlando, 1986
11. Cannon J, Stoll J, Knowles H et al: Realtime three-dimensional ultrasound for guiding surgical task. Compute Aided Surg, 2003; 8: 82–90
12. Gee A, Prager R, Treece G: Processing and visualizing three-dimensional ultrasound data. Br J Radiol, 2004; 77: S186–93
13. Watanabe M, Kida M, Yamada Y et al: Measuring tumor volume with three-dimensional endoscopic ultrasonography: an experimental and clinical study. Endoscopy, 2004; 36: 976–81
14. Castelman D: Digital image processing. Prentice Hall, Upper Saddle River, 1996
15. Suri J, Saterehdan S, Singh S (eds.): Advanced algorithmic approaches to medical image segmentation. Springer, London, 2002
16. Zimmer Y, Tepper R, Akselrod S: A two-dimensional extension of minimum cross entropy thresholding for the segmentation of ultrasound images. Ultrasound Med Biol, 1996; 22: 1183–90
17. Ross P, Menu Y, Vilgrain V: Liver neoplasms and tumor-like conditions. Eur Radiol, 2001; 11: S145–65
18. Petrick N, Chan H, Sahiner S et al: An adaptive density-weighted contrast enhancement filter for mammographic breast mass detection. IEEE Trans Med Imag, 1996; 19: 59–67
19. Qian W, Clarke L: Image feature extraction for mass detection in digital mammography: influence of wavelet transform. Med Phys, 1999; 26: 402–8
20. Kadah Y, Farag A, Zurada J et al: Classification algorithms for quantitative tissue characterization of diffuse liver disease from ultrasound images. IEEE Trans Med Imag, 1996; 15: 466–78
21. Mojsilovic A, Popovic M, Meskovic A: Wavelet image extension for analysis and classification of infrared myocardial tissue. IEEE Trans Biomed Eng, 1997; 44: 856–66
22. Scheipers U, Ermert H, Sommerfeld H et al: Ultrasonic multifeature tissue characterization for prostate diagnosis. Ultrasound Med Biol, 2003; 29: 1137–49
23. Chappard D, Guggenbuhl, Legrand E et al: Texture analysis of X-ray radiographs in correlated with bone histomorphometry. J Bone Miner Metab, 2005; 23: 24–29
24. McLachlan G: Discriminant analysis and statistical pattern recognition. Hohn Willey & Sons, New York, 1992
25. Valckx F, Thijssen J: Characterization of echographic image texture by cooccurrence matrix parameters. Ultrasound Med Biol, 1997; 23: 559–71
26. Thijssen J, Oosterveld B, Hartmann P et al: Correlations between acoustic and texture parameters from rf- and B-mode liver echograms. Ultrasound Med Biol, 1993; 19: 13–23
27. Parkinnen J, Selkainaho K: Detecting texture periodicity from the co-occurrence matrix. Pattern Recognition Lett, 1990; 11: 43–50